# Characterization and Dynamics of Aggresome Formation by a Cytosolic GFP-Chimera

**Rafael García-Mata,* Zsuzsa Bebök,‡ Eric J. Sorscher,‡ and Elizabeth S. Sztul***

*Department of Cell Biology, University of Alabama at Birmingham, Birmingham, Alabama 35294; and ‡The Gregory Fleming James Cystic Fibrosis Research Center, University of Alabama at Birmingham, Birmingham, Alabama 35294

***Abstract.*** Formation of a novel structure, the aggresome, has been proposed to represent a general cellular response to the presence of misfolded proteins (Johnston, J.A., C.L. Ward, and R.R. Kopito. 1998. *J. Cell Biol.* 143:1883–1898; Wigley, W.C., R.P. Fabunmi, M.G. Lee, C.R. Marino, S. Muallem, G.N. DeMartino, and P.J. Thomas. 1999. *J. Cell Biol.* 145:481–490). To test the generality of this finding and characterize aspects of aggresome composition and its formation, we investigated the effects of overexpressing a cytosolic protein chimera (GFP-250) in cells. Overexpression of GFP-250 caused formation of aggresomes and was paralleled by the redistribution of the intermediate filament protein vimentin as well as by the recruitment of the proteasome, and the Hsp70 and the chaperonin systems of chaperones. Interestingly, GFP-250 within the aggresome appeared not to be ubiquitinated. In vivo time-lapse analysis of aggresome dynamics showed that small aggregates form within the periphery of the cell and travel on microtubules to the MTOC region where they remain as distinct but closely apposed particulate structures. Overexpression of p50/dynamitin, which causes the dissociation of the dynactin complex, significantly inhibited the formation of aggresomes, suggesting that the minus-end–directed motor activities of cytoplasmic dynein are required for aggresome formation. Perinuclear aggresomes interfered with correct Golgi localization and disrupted the normal astral distribution of microtubules. However, ER-to-Golgi protein transport occurred normally in aggresome containing cells. Our results suggest that aggresomes can be formed by soluble, nonubiquitinated proteins as well as by integral transmembrane ubiquitinated ones, supporting the hypothesis that aggresome formation might be a general cellular response to the presence of misfolded proteins.

Key words: aggresome • p50/dynamitin • chaperones • proteasome • microtubules

Newly synthesized cellular proteins fold by a process in which the linear information contained in a chain of amino acids is converted into a functional three-dimensional structure. It has been established that small monomer proteins fold through a succession of a definite number of intermediate steps (Jaenicke, 1991). In cells, misfolding can occur due to particular arrangements of linear amino acids or mutations within the protein, outside stresses, or unequal synthesis of individual subunits of multiunit proteins (Bonifacino et al., 1989; Morimoto et al., 1990; Hurle et al., 1994; Ward and Kopito, 1994). Misfolded proteins often expose hydrophobic domains, which can lead to nonproductive association and protein aggregation (Wetzel, 1994). Protein aggregation has been regarded usually as a curiosity arising in artificial in vitro systems. However, there is a growing body of evidence suggesting that aggregation of newly synthesized polypeptides can also be a problem in vivo (Wetzel, 1994). Specifically, the deposition of misfolded proteins in cellular aggregates has been linked to the pathogenesis of many diseases (Carrel and Lomas, 1997). In humans, Alzheimer's disease and other types of amyloidosis involve the formation of highly insoluble protein aggregates within neuronal cells (Sipe, 1992; Thomas et al., 1995).

The fate of a polypeptide, i.e., whether it folds into its native functional state or forms aggregates, is determined by competition between folding, degradation, and aggregation. In cells synthesizing large amounts of a heterologous protein, aggregation may be amplified by the high concentration of identical nascent chains emerging from polysomes, and by the very large increases in association constants produced by the crowding effect of the high concentration of macromolecules in the cytoplasm (Zimmermann and Minton, 1993; Ellis and Hartl, 1996; Dobson

The online version of this article contains supplemental material.

Address correspondence to Elizabeth Sztul, Department of Cell Biology, MCLM, Room 668, 1918 University Boulevard, Birmingham, AL 35294. Tel.: (205) 934-1465. Fax: (205) 975-9131. E-mail: esztul@uab.edu

and Ellis, 1998). Other factors like pH, temperature, ionic strength, and redox environment, or inhibition of specific degradative pathways can also produce folding intermediates with the potential to form aggregates.

Recently, it has been shown that when production of misfolded proteins exceeds the cellular capacity to degrade them, the proteins accumulate in a novel subcellular structure, the aggresome (Johnston et al., 1998). Overexpression of the inefficiently folded cystic fibrosis transmembrane conductance regulator (CFTR)[1] or inhibition of proteasome activity in cells expressing CFTR led to the accumulation of stable, ubiquitinated aggregates of CFTR. The same phenomenon was observed when another transmembrane protein, presenilin-1 (PS1), was overexpressed in cells in which proteasome function was inhibited (Johnston et al., 1998). The misfolded proteins were deposited in large aggregates surrounding the MTOC and ensheathed in a cage of vimentin. The structure was termed the aggresome, and it was proposed that the formation of an aggresome is a general cellular response to the presence of aggregated, nondegraded proteins. While this manuscript was under review, a report describing a similar phenomenon appeared and demonstrated that even under basal conditions, the proteasome, ubiquitin, Hsp70, and Hsp90 concentrate in the MTOC (Wigley et al., 1999). This structure enlarges in response to inhibition of the proteasome and to overexpression of CFTR, and recruits the cytosolic pools of ubiquitin and the proteasome. Although aggresome deposition has been proposed to represent a general response, so far, only misfolded transmembrane proteins have been shown to be involved in this phenomenon. Consequently, we set out to test the generality of this finding and further characterize aspects of aggresome formation and composition.

In this study, we investigated the formation of an aggresome by a protein chimera (GFP-250) composed of the entire soluble protein GFP fused at its COOH terminus to a 250–amino acid fragment of the cytosolic protein, p115. p115 is a membrane transport actor, peripherally associated with membranes, and has been localized to the Golgi (Waters et al., 1992; Nakamura et al., 1997) and to transport intermediates carrying cargo from the ER to the Golgi (vesicular tubular clusters or VTCs) (Nelson et al., 1998). Here, we show that overexpression of GFP-250 caused formation of aggresomes morphologically indistinguishable from those formed by CFTR or PS1. Aggresome formation by GFP-250 did not require proteasome inhibition, and large aggresomes formed spontaneously in >50% of the transfected cells 48 h after transfection. The proteasome was recruited to the aggresomal region and appeared to be responsible for the degradation of GFP-250. In contrast to the previous report (Johnston et al., 1998), GFP-250 appeared not to be ubiquitinated. Formation of GFP-250 containing aggresome was paralleled by the recruitment of a vimentin cage and of the Hsp70 and the chaperonin systems of chaperones to the aggresome in a spatially distinct manner. Time-lapse image analysis in living cells was used to characterize the dynamics of aggresome formation. Our data suggest that small aggregates form peripherally and travel on microtubules in a minus-end direction to the MTOC region where they remain as distinct but closely apposed particulate structures. Overexpression of p50/dynamitin significantly reduced the extent of aggresome formation, suggesting that dynein/dynactin is involved in this minus-end–directed movement. Aggresome formation interfered with correct Golgi localization and disrupted the normal astral distribution of microtubules. However, despite these structural problems, membrane transport from the ER to the Golgi occurred normally in aggresome containing cells. Taken together, our results provide support for the hypothesis that aggresome formation might be a general cellular response to the presence of misfolded proteins by demonstrating that this response can involve cytosolic, nonubiquitinated proteins as well as transmembrane ubiquitinated ones, and extend the previous findings by characterizing the dynamics of aggresome formation and the nature of the motors involved in its formation.

## Materials and Methods

### Antibodies and Reagents

Anti–*Aquorea victoria* GFP rabbit polyclonal antibody, Texas red–conjugated goat anti–rabbit and anti–mouse antibodies, and AMCA-S–conjugated goat anti–mouse antibodies were purchased from Molecular Probes. Anti-p115 polyclonal antibody was as described previously (Nelson et al., 1998). Anti-Hsc70, anti-Hdj1, anti-Hdj2, anti-TCP1, and polyclonal anti-ubiquitin were a generous gift from Dr. Douglas Cyr (University of Alabama at Birmingham). Anti-giantin antibody was a gift from Dr. Hans P. Hauri (University of Basel, Switzerland). Anti-ubiquitin monoclonal antibody and anti-20S proteasome (α-subunit) polyclonal antibody were purchased from Calbiochem-Novabiochem. Anti-β-tubulin monoclonal antibody and nocodazole were purchased from Sigma Chemical Co. Monoclonal anti-VSV-G was a gift from Dr. Kathryn Howell (University of Colorado). Nocodazole was used at a concentration of 10 μg/μl. *Clasto*-lactacystin β-lactone (Calbiochem-Novabiochem) was used at a concentration of 10 μM. Monoclonal anti-p50 (mAb 50.1) was a gift from Dr. Richard B. Vallee (University of Massachusetts Medical School). Anti-vimentin monoclonal antibody was a gift from Dr. Bill Britt (University of Alabama at Birmingham).

### DNA Constructs

To make the different GFP chimeras used in this study, polymerase chain reaction (PCR) was used to introduce restriction sites at the $NH_2$ terminus (XhoI) and at different sites downstream (BamHI) of the p115 cDNA previously described (Barroso et al., 1995). The PCR products were then digested and subcloned in pEGFP-C2 vector (Clontech). pcDNA3.1 (Invitrogen) containing wild-type CFTR was used for CFTR expression in mammalian cells. The plasmid used for p50 expression (pCMVH50myc) (Echeverri et al., 1996) was a gift from Dr. Richard B. Vallee (University of Massachusetts Medical School).

### Cell Culture and Transfection

COS-7 cells were grown in DME supplemented with 10% FBS and 100 U/ml penicillin, 100 μg/ml streptomycin at 37°C in 5% $CO_2$. Cells growing on 12-mm coverslips were transiently transfected using a calcium phosphate transfection system (GIBCO BRL). After 24 h, cells were washed once with PBS and then incubated in complete medium for an additional 24 h. Cells were imaged live on a temperature-controlled microscope at 37°C. pcDNA-wtCFTR was transfected into COS-7 cells using Lipofectamine-Plus (GIBCO BRL) according to the manufacturer's instructions.

1. *Abbreviations used in this paper:* CFTR, cystic fibrosis conductance transmembrane regulator; MT, microtubule; MTOC, microtubule organizing center; PS1, presenilin 1; ROI, region of interest; VSV, vesicular stomatitis virus.

### Analysis of Soluble and Insoluble Fractions

COS-7 cells were either mock transfected or transfected with GFP-250. 48 h after transfection, cells were washed with ice-cold PBS and collected by trypsinization. Each pellet was washed three times with PBS and resuspended with PBS supplemented with a mammalian protease inhibitor cocktail (Sigma). Cell pellets were then washed twice with PBS and lysed for 30 min on ice with 200 μl of either 2% Triton X-100 in PBS, IPB (10 mM Tris-HCl, pH 7.5, 5 mM EDTA, 1% NP-40, 0.5% deoxycholate, and 150 mM NaCl), or RIPA buffer (50 mM Tris-HCl, pH 8, 1% NP-40, 0.5% deoxycholate, 0.1% SDS, and 150 mM NaCl), all supplemented with protease inhibitor cocktail. Lysates were then passed 10 times through a 27-gauge needle. Insoluble material was recovered by centrifugation at 13,000 *g* for 15 min at 4°C. Pellets were then resuspended in 200 μl of 1% SDS in PBS and sonicated for 20 s with a microtip sonicator. Equal volumes of each pellet and supernatants were boiled for 5 min in SDS-PAGE sample buffer and analyzed by SDS-PAGE.

### Analysis of tsO45 VSV-G Transport

COS-7 cells grown on coverslips were infected with the temperature sensitive strain of the vesicular stomatitis virus (tsO45 VSV) at 32°C for 30 min. Cells were then shifted to 42°C for 3 h to accumulate the misfolded G protein in the ER. Transport of G protein was initiated by incubating the cells at 32°C. After 1 h, cells were fixed and processed for indirect immunofluorescence.

### Immunoblotting

Samples were separated by SDS-PAGE, transferred to nitrocellulose membranes, and analyzed by immunoblotting with the indicated antibodies. To remove primary and secondary antibodies, membranes were incubated for 30 min in stripping buffer (100 mM 2-mercaptoethanol, 2% SDS, 62.5 mM Tris-HCl, pH 6.7) at 50°C and washed twice with PBS; 0.2% Tween 20. Membranes were then incubated with the detection reagent (ECL; Amersham Life Science Ltd.) to ensure the removal of antibodies, washed, and reprobed with the antibody indicated.

### Metabolic Radiolabeling and Immunoprecipitation

COS-7 cells were transfected with GFP-250 for 12 h. Cells were then washed in PBS and incubated in methionine-free DMEM for 1 h. One well of a six-well tissue culture plate ($\sim 2 \times 10^6$ cells) was used per sample. Cells were labeled with 200 μCi [$^{35}$S]methionine (NEN, Life Science Products) for 60 min. Incorporation was terminated by washing the cells with PBS and replacing the media with nonradioactive DMEM (methionine). Direct immunoprecipitation was carried out after lysing the cells in RIPA buffer. The cells were scraped, lysed for 30 min on ice, and then centrifuged at 14,000 rpm for 10 min. Immunoprecipitation was for 2 h at 4°C using anti-p115 polyclonal antibody and protein A agarose. Proteins were washed and separated by SDS-PAGE on a 10% gel. Gels were vacuum dried and labeled proteins were detected by fluorography and analyzed using IPLab Spectrum software (Signal Analytics).

### Immunofluorescence Microscopy

Cells grown on coverslips were washed three times in PBS and fixed in 3% paraformaldehyde in PBS for 10 min at room temperature. Paraformaldehyde was quenched with 10 mM ammonium chloride. For chaperones staining, cells were fixed for 10 min with methanol at –20°C as previously described (Meacham et al., 1999). Cells were permeabilized with 0.1% Triton X-100 in PBS for 7 min at room temperature. The coverslips were then washed three times for 2 min each with PBS and then blocked in PBS, 2.5% goat serum, and 0.2% Tween 20 for 5 min followed blocking in PBS, 0.4% fish skin gelatin, and 0.2% Tween 20. Cells were incubated with primary antibody diluted in PBS, 0.4% fish skin gelatin, 0.2% Tween 20 for 45 min at 37°C. Coverslips were washed five times for 5 min each with PBS and 0.2% Tween 20. Secondary antibodies were diluted in PBS, 2.5% goat serum, and 0.2% Tween 20, and incubated on coverslips for 30 min at 37°C. Coverslips were washed as above and mounted on slides in 9:1 glycerol/PBS with 0.1% p-phenylenediamine.

### Electron Microscopy

COS-7 cells were transfected with GFP-250. After 48 h, cells were washed with PBS, collected by trypsinization and pelleted in a microfuge at 4°C. The pellet was washed twice with PBS and then fixed for 90 min with 1.5% glutaraldehyde in 0.1 M sodium cacodylate pH 7.4. Cells were washed three times with sodium cacodylate and postfixed in $OsO_4$ in 0.1 M sodium cacodylate pH 7.4 for 60 min on ice. After washing three times with sodium cacodylate 0.1 M, cells were subjected to a series of graded ethanol dehydration (30, 50, 70, 90, 95, 100%) followed by 1 h incubation in 1:1 100% ethanol/Polybed resin (Polysciences, Inc.). After two changes of fresh 100% resin, the cell pellets were transfected to gelatin molds and polymerized in fresh resin overnight at 60°C. Gold epoxy sections (100 nm thick) were generated with a Reichert Ultracut ultramicrotome and collected on 200 mesh copper grids. The grid specimens were then stained for 20 min with saturated aqueous uranyl acetate (3.5%) diluted 1:1 with ethanol just before use, followed by staining with lead citrate for 10 min. Stained samples were subsequently examined on a JEOL 100CX electron microscope.

### Time-Lapse Imaging and Microscopy

COS-7 cells grown on glass coverslips were sealed into a silicon rubber chamber placed on a glass slide and containing buffered medium with Hepes 25 mM, pH 7.5. Images were acquired in a Zeiss Axiovert 30 inverted microscope (Carl Zeiss Inc.). The microscope was equipped with a 100×, 1.4 NA objective (Carl Zeiss Inc.) and a cooled charge-coupled device (Photometrics) for 12 bit detection. IpLab Spectrum software (Signal Analytics) was used to control image acquisition and manipulation. Deconvoluted images were obtained by collecting images on an OlympusIX70 inverted microscope with a 40×/1.35 NA objective and deconvoluted using IPLab software (Signal Analytics). 4 μm of optical sections 0.4 μm thick was analyzed.

### Online Supplemental Material

Figure 8 A: Dynamics of aggresome formation in vivo. Individual frames collected every 60 s for a period of 2 h. Frames corresponding to time points 60–120 min were exported to a movie file using QuickTime™ 3.0 software. Video available at http://www.jcb.org/cgi/content/full/146/6/1239/F8/DC1

## Results

### Expression of a Cytosolic Protein Chimera Causes Formation of Aggresomes

GFP has been extensively and successfully used as a fusion partner to host proteins to monitor their intracellular localization and fate (reviewed in Tsien, 1998). The ideal chimera is a protein that preserves all the targeting and physiological functions and localization of the host protein but is now fluorescent. GFP-tagged chimeric proteins have been targeted successfully to practically every major organelle of the cell (reviewed in Tsien, 1998). Because each GFP represents one fluorophore, relatively high levels of expression are required to give bright signals. Several GFP constructs have been expressed at high levels without affecting proper localization and function (Marshall et al., 1995; Carey et al., 1996; Rizzuto et al., 1996; Presley et al., 1997). However, nonsuccessful fusions are almost never published, making it very difficult to know if overexpression of a specific chimera can trigger an abnormal cellular response (Cubbit et al., 1995).

We have shown previously that the wild-type peripherally membrane-associated transport factor p115 localizes to the Golgi complex and to VTCs in interphase cells (Nelson et al., 1998). Similarly, when a GFP chimera containing full-length p115 fused to the COOH terminus of GFP was expressed in COS-7 cells, the fusion protein localized to the Golgi complex as shown by a high degree of colocalization with the Golgi marker giantin (Linstedt and Hauri, 1993) (Fig. 1, A and B). p115 contains 959 amino acids or-

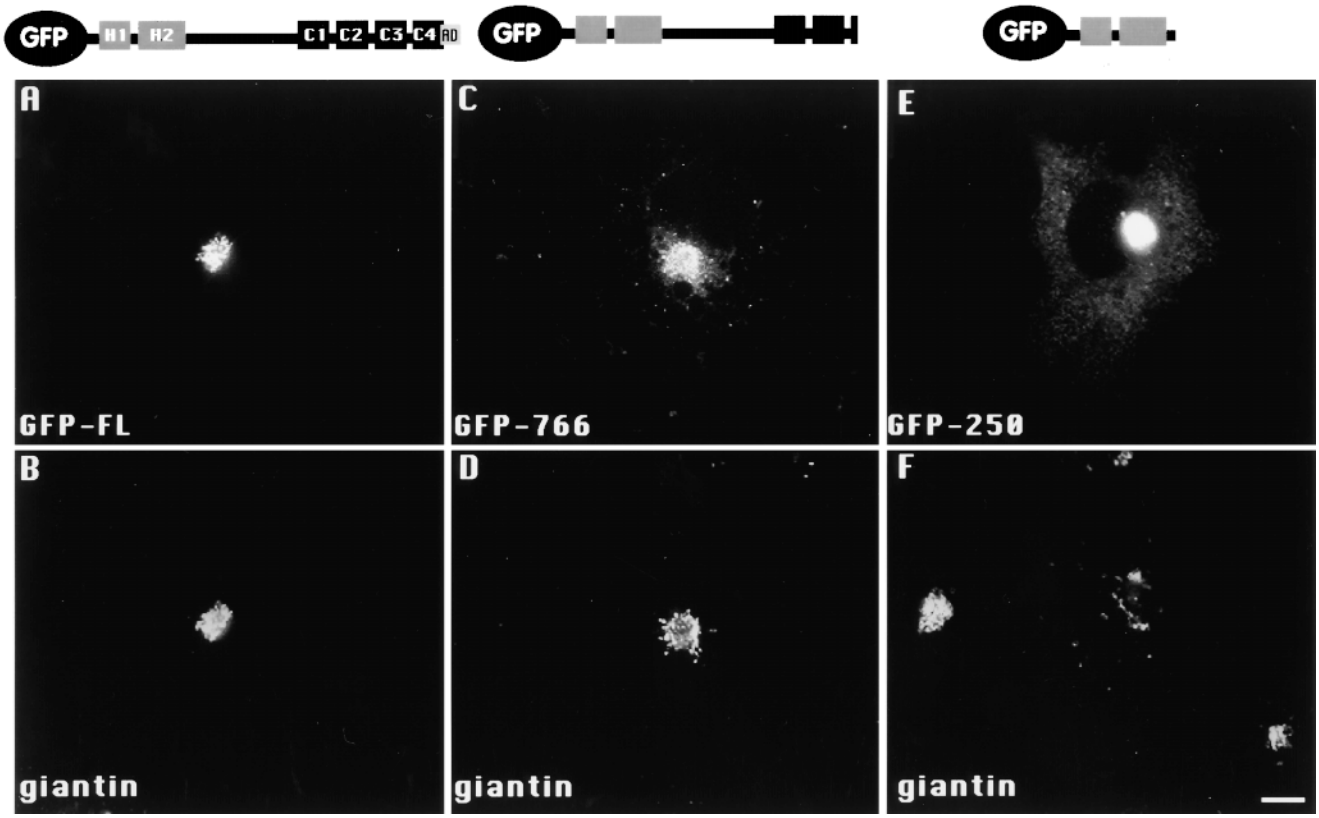


*Figure 1.* Overexpression of a cytosolic protein leads to aggresome formation. COS-7 cells were transfected with chimeras between GFP and various domains of p115. A schematic representation of each chimeric protein used in the transfections is shown above each panel; GFP, green fluorescent protein; H1 and H2, domains within p115 highly homologous to Uso1p; C1-4, predicted p115 coiled-coil regions; AD, p115 acidic domain. 48 h after transfection, cells were processed for immunofluorescence using anti-giantin antibodies. Chimeras containing full-length p115 (GFP-FL; A and B) or lacking a small region of the COOH terminus (GFP-766; C and D) colocalized with giantin in the Golgi region. The chimera containing only the $NH_2$-terminal H1 and H2 region of p115 (GFP-250; E and F) localized to a perinuclear structure surrounded by displaced Golgi elements. Bar, 10 μm.

ganized into a globular head containing two domains (H1 and H2) with strong homology to a yeast protein Uso1p and a tail domain containing four coiled-coil (C1-C4) segments (Barroso at al., 1995; Sapperstein et al., 1995). At the COOH terminus, p115 contains a conserved acidic domain (AD). Eliminating the COOH-terminal region of the GFP full-length p115 chimera by removing the COOH-terminal acidic domain, coil 4, and a portion of coil 3 of p115, generated a construct with a normal Golgi localization (Fig. 1, C and D). In contrast, when COS-7 cells were transfected with a GFP chimera consisting of GFP fused to the $NH_2$-terminal first 252 amino acids of p115 (GFP-250), the construct did not colocalize with the Golgi marker giantin (Fig. 1, E and F). After 48 h of transfection, ~50% of transfected cells showed majority of the GFP signal concentrated in a single large circular structure localized close to one side of the nucleus. In addition, in most cells, GFP fluorescence was also detected in small punctate structures scattered throughout the periphery of the cells. The finding that normal Golgi morphology appears disrupted in cells containing this perinuclear structure (Fig. 1, E and F) will be discussed later.

To examine if the targeting of the GFP-250 chimera to the perinuclear structure was dependent on the position of the GFP within the chimera, we tested the localization of a construct containing the same fragment of p115 as GFP-250, but with the GFP fused to its COOH terminus (250-GFP). Interestingly, overexpression of 250-GFP construct did not cause the formation of the perinuclear structure (compare Fig. 2, A and B), nor did overexpression of the vector alone (Fig. 2 C). Overexpression of either 250-GFP or GFP gave a diffuse pattern suggesting cytosolic and nuclear localization as previously shown for GFP (Kain et al., 1995; Ogawa et al., 1995). Therefore, it appears that only a specific arrangement of protein sequences results in a protein that is deposited in the perinuclear structures. In data to be presented, we show that GFP-250 is present in insoluble aggregates. However, it is important to note that even though misfolding is likely to be involved in the mechanism of GFP-250 aggregation, the GFP moiety of the chimera must be properly folded, since green fluorescence is detected in these studies.

The large perinuclear structure containing GFP-250 showed striking similarity to a recently described novel subcellular compartment, the aggresome (Johnston et al., 1998). As previously reported, overexpression of the poly-

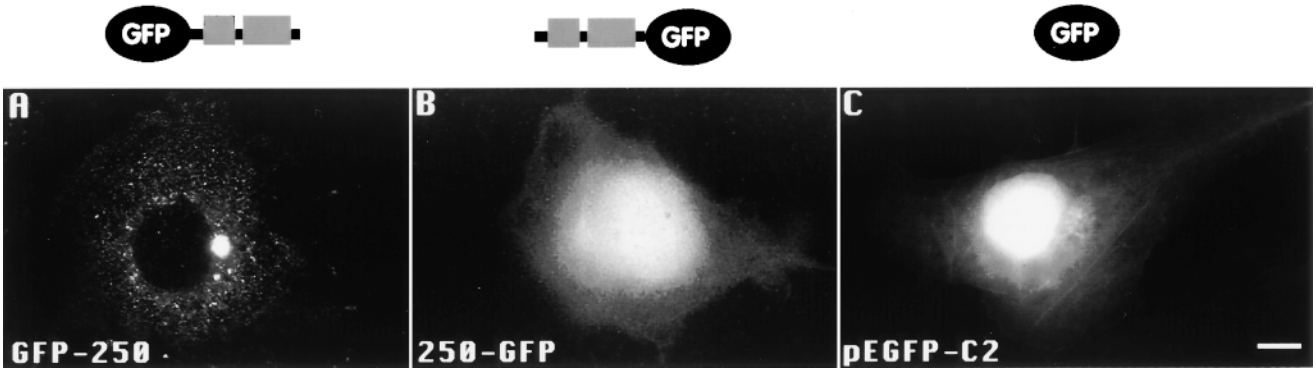


*Figure 2.* Aggresome formation depends on the position of the GFP within the chimera. COS-7 cells were transfected with the indicated GFP chimeras or with GFP alone. The region of p115 within the constructs is the same as in Fig. 1 in GFP-250. 48 h after transfection, cells were imaged for GFP. Only the chimera containing GFP at the $NH_2$ terminus (A) formed an aggresome, whereas the chimera containing GFP at the COOH terminus (B) or GFP alone (C) did not form an aggresome. Bar, 10 μm.

topic membrane protein CFTR or inhibition of proteasome activity in cells expressing CFTR leads to the accumulation of stable CFTR aggregates in a large structure close to the MTOC region. To further characterize the structures formed by GFP-250, we examined GFP-250 transfected cells by electron microscopy. The efficiency of transfection was usually close to 40% and a significant proportion, usually >50% of transfected cells, contained a single large perinuclear structure when analyzed by fluorescence (analogous to that seen in Fig. 1 E). At the ultrastructural level, transfected cells contained a relatively large (~4 μm) rounded structure of electron-dense particles adjoining the nucleus (Fig. 3 A). The structure was composed of individual dense particles, ~50–90 nm in size (Fig. 3 B), analogous to the 60–80-nm particles reported to contain misfolded CFTR (Johnston et al., 1998). Membranous organelles were detected within the particulate structure and surrounding the aggregate (Fig. 3 B). The aggregate shown in Fig. 3 is surrounding one of the centrioles (arrowhead in Fig. 3 B), indicating that it formed around the MTOC. At higher magnification, long filaments can be seen surrounding the aggregate (asterisk in Fig. 3 C). Aggresome formation by CFTR caused a redistribution of the intermediate filament protein vimentin to the aggresomal region forming a cage-like structure (Johnston et al., 1998). Overexpression of GFP-250 elicited the same response as determined by indirect immunofluorescence using anti-vimentin antibodies. As shown in Fig. 4, vimentin forms a ring around the aggregated GFP-250 (Fig. 4 A), that surrounds the aggregated protein core (Fig. 4 B). These findings suggest that overexpression of a cytosolic protein can also trigger aggresome formation.

### *Cytosolic Chaperones Are Recruited to Aggresomes*

Molecular chaperones bind to and stabilize aggregation-sensitive proteins and facilitate their ultimate fate, be it folding, assembly, transport to a particular subcellular compartment, or disposal by degradation (reviewed in Hartl, 1996). In a recent report, Hsp70 and Hsp90 have been shown to be recruited to the centrosomal region upon inhibition of the proteasome (Wigley et al., 1999). Since aggresomes contain misfolded proteins destined for degradation, it might be expected that such polypeptides could be complexed with specific chaperones. To determine if distinct classes of molecular chaperones are associated with the aggresome, indirect immunofluorescence was used to determine the localization of four different cytosolic chaperones in GFP-250–transfected cells. Localization of three chaperones of the Hsp70 system (Hsc70, and two Hsp40 members, Hdj1 and Hdj2) and of one chaperonin (TCP1) was examined. As shown in Fig. 5, of the four molecules tested, three (Hdj1, Hdj2, and TCP1) showed a high degree of colocalization with GFP-250 within the aggresome. Interestingly, Hsc70 was restricted to the periphery of the aggresome forming a ring around the GFP-250 signal. The restricted localization of Hsc70 to the periphery of the aggresome is perplexing since Hsc70 participates in protein folding events in conjunction with a matching member of the Hsp40 family, Hdj1 or Hdj2 (Cyr, 1997; Frydman and Hohfeld, 1997; Hohfeld and Jentsch, 1997; Takayama et al., 1997; Meacham et al., 1999). The differential localization might suggest that Hsc70 chaperone is recruited later in the process of the aggresome formation, or that it is associated with vimentin surrounding the aggresome, but not with the aggregated particles. Supporting the latter possibility, Hsc70 colocalized with vimentin in a ring structure around the aggresome (Fig. 5 B).

### *The 20S Proteasome Is Recruited to the Aggresome and Is Responsible for GFP-250 Degradation*

The proteasome has been implicated in the degradation of incompletely folded or misfolded proteins (Kopito, 1997). In the case of CFTR, both the mutant forms and up to 70% of the wild-type protein fail to fold correctly and are eliminated by an ATP-dependent process that requires covalent modification with ubiquitin and degradation by the proteasome (Jensen et al., 1995; Ward et al., 1995). Similarly, Wigley et al. (1999) reported the recruitment of the proteasomal machinery to the centrosome in cells overexpressing CFTR. To determine if the GFP-250 aggresome also recruited the proteasome, we analyzed the distribu-

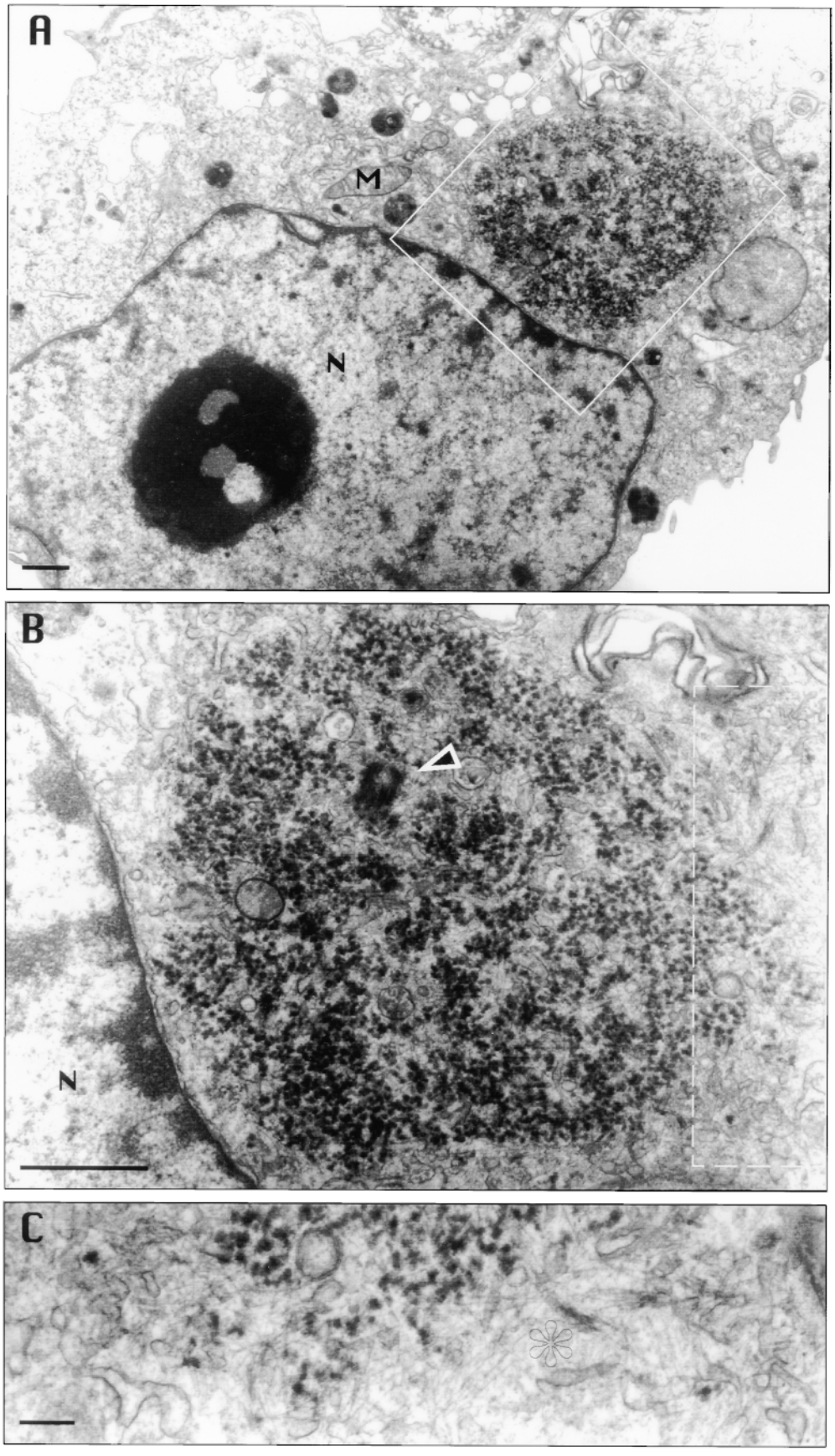


*Figure 3.* Ultrastructural analysis of GFP-250–transfected cells. COS-7 cells were transfected with GFP-250, and processed for electron microscopy 48 h later. An aggregate of particulate material is seen close to the nucleus (A). A higher magnification of the material (B) shows that it surrounds a centriole (arrowhead) and is surrounded by filamentous material (dashed rectangle). The filamentous material appears to be composed of 10-nm filaments (asterisk in C). M, mitochondria; N, nucleus. Bars: (A and B) 1 μm; (C) 0.25 μm.

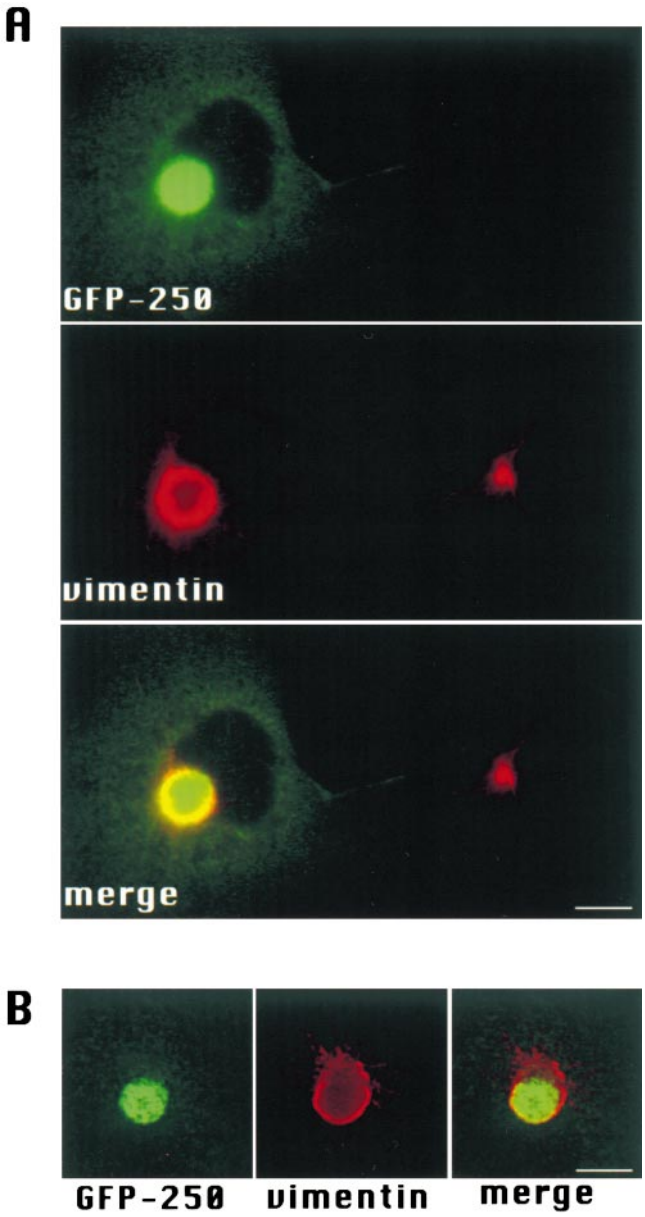


*Figure 4.* Aggresome formation causes a redistribution of the intermediate filament protein vimentin. COS-7 cells were transfected with GFP-250. 48 h after transfection, cells were processed for immunofluorescence using anti-vimentin antibodies and imaged to localize the GFP-250 and the vimentin. Images in A were acquired using conventional optics. Images in B are deconvoluted 0.4-μm optical sections. Vimentin is recruited into a ring structure around the aggresome. Bars, 10 μm.

tion of the α-subunit of the 20S proteasome in GFP-250–expressing cells. As shown in Fig. 6 A, the proteasome is localized to the GFP-250 aggresome, suggesting that it may be involved in the degradation of GFP-250. To examine this directly, COS-7 cells were transfected with the GFP-250 chimera and after 36 h were incubated with the proteasome inhibitor *clasto*-lactacystin β-lactone for 11 h. Cells were then fixed and examined for green fluorescence to determine the percentage of transfected cells that formed an aggresome. A parallel experiment was performed in the absence of the proteasome inhibitor. As shown in Fig. 6 B, ~53% of control cells (700 cells counted) formed an aggresome, whereas ~88% of cells treated with the proteasome inhibitor (700 cells counted) formed an aggresome. To confirm that the proteasome is involved in the degradation of GFP-250, COS-7 cells transfected with GFP-250 were subjected to pulse–chase analysis in the presence or absence of *clasto*-lactacystin β-lactone. Fig. 6 C shows that the stability of the radiolabeled GFP-250 increases approximately twofold in the presence of the inhibitor. These results suggest that the proteasome is recruited to the GFP-250 aggresome and plays a key role in the degradation of GFP-250.

### *GFP-250 within Aggresomes Appears Nonubiquitinated*

It has been shown previously that inhibiting the activity of the 20S proteasome and/or overexpressing of CFTR or CFTR mutants induce the accumulation of multiubiquitinated detergent-insoluble forms of the proteins (Ward et al., 1995). To examine the solubility of GFP-250, increasingly stringent solubilization methods were used. As shown in Fig. 7 A, even under the most stringent conditions using Triton X-100 and SDS (RIPA buffer), GFP-250 was only detected in the insoluble fraction. In contrast, β-tubulin was detected only in the soluble fraction under all solubilization conditions, suggesting that the extraction methods efficiently disrupted the microtubule cytoskeleton.

The usual characteristic of polyubiquitination is a ladder of bands spaced by ~7-kD intervals or the appearance of a high molecular mass smear in an SDS gel, both of which reflect the covalent attachment of multiple ubiquitin chains to the target protein (for example see Glotzer et al., 1991; Ward et al., 1995). The ubiquitination serves as a proteasome degradation signal for the target protein (reviewed by Hershko and Ciechanover, 1998). The aggresomes formed in cells with inhibited proteasome contained CFTR conjugated to ubiquitin (Johnston et al., 1998). To examine if aggresomes formed by overexpression of GFP-250 contained polyubiquitinated GFP-250, transfected COS-7 cells were separated into Triton X-100–soluble and –insoluble fractions, and immunoblotted with an antibody raised against GFP. As shown in Fig. 7 B, a single band with the molecular mass (~55 kD) predicted for GFP-250 was detected in the detergent-insoluble fraction. Higher molecular mass bands or a high molecular mass smear were not detected, suggesting that the aggregated GFP-250 chimera was not ubiquitinated. To confirm this finding, the nitrocellulose membrane was stripped and reprobed with polyclonal antibodies raised against ubiquitin. As shown in the ubiquitin-probed panel, multiple bands were detected in the soluble and the insoluble fractions. A major band of ~65 kD, few minor bands as well as a smear comprising a wide range of molecular masses is detected in the soluble fraction. A single major band of ~35 kD is detected in the insoluble fraction, but does not correspond to the molecular mass of GFP-250. These results suggest that GFP-250 is not ubiquitinated to a detectable extend.

Ubiquitination of some substrates appears labile and to confirm that GFP-250 present within the aggresome is not

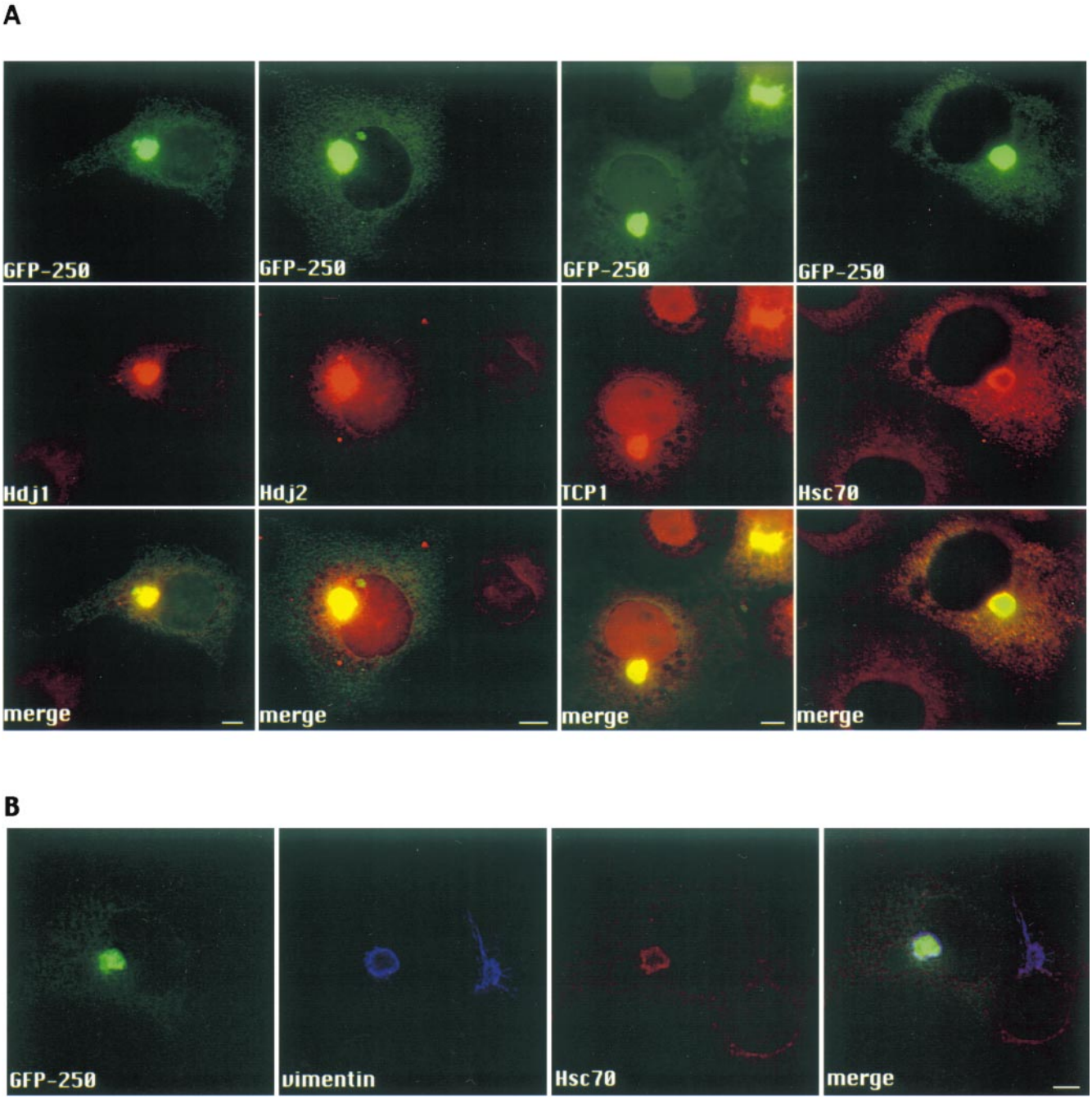


*Figure 5.* Cytosolic chaperones are recruited to the aggresome. COS-7 cells were transfected with GFP-250. (A) 48 h after transfection, cells were processed for immunofluorescence using antibodies to Hdj1, Hdj2, Hsc70, and TCP1, and imaged to localize the GFP chimera and the chaperone. (B) 48 h after transfection, cells were processed for immunofluorescence using antibodies to Hsc70 and vimentin, and imaged to localize the GFP-250, Hsc70, and vimentin. Hdj1, Hdj2, and TCP1 colocalize with the aggresome, while Hsc70 forms a ring around the aggresome. Vimentin colocalizes with the ring of Hsc70. Images in B are deconvoluted 0.4-μm optical sections. Bars, 10 μm.

ubiquitinated, we examined COS-7 cells transfected with GFP-250 and processed by immunofluorescence with antibodies to ubiquitin. As shown in Fig. 7 C, the GFP-250 containing aggresome showed no significant colocalization with ubiquitin, which showed a dispersed punctate staining throughout the cell. To ensure that the anti-ubiquitin antibodies can react with ubiquitin in this assay, we transfected COS-7 cells with CFTR since ubiquitin has been shown to colocalize with CFTR in the aggresomal region in proteasome-inhibited cells (Johnston et al., 1998). After 36 h of transfection with CFTR, cells were treated overnight with *clasto*-lactacystin β-lactone to induce aggresome formation. The cells were then fixed and processed by immunofluorescence with antibodies to CFTR and

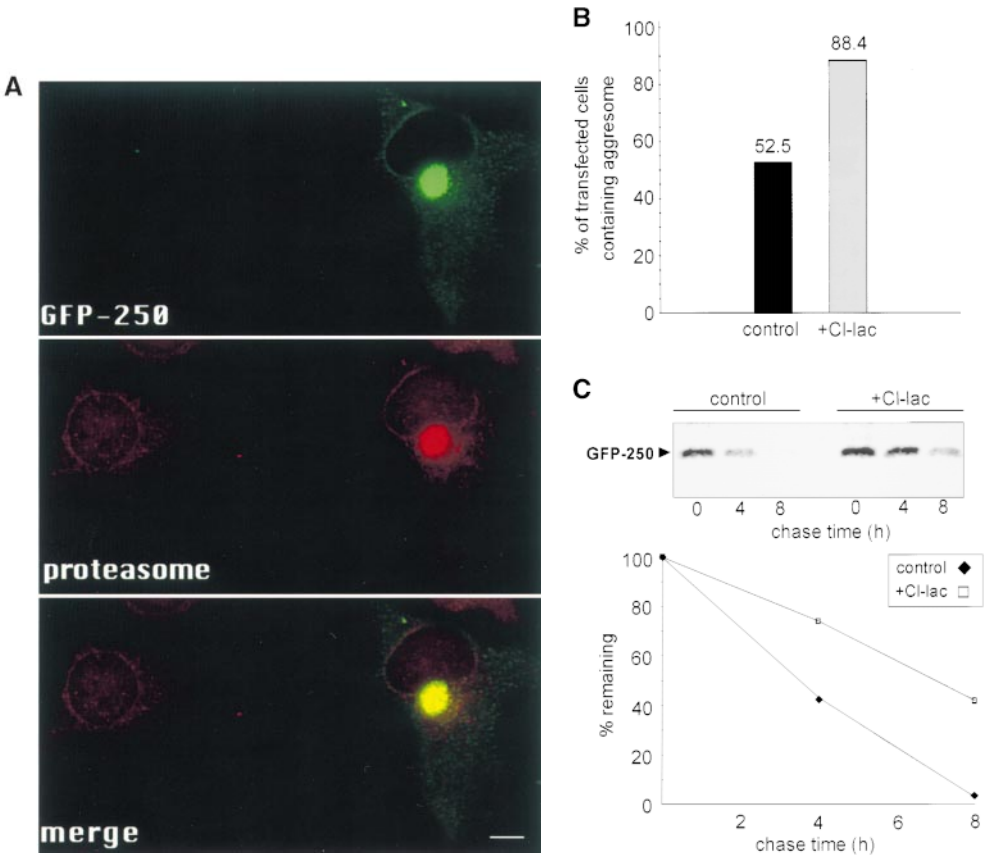


*Figure 6.* The proteasome is recruited to the aggresome and is responsible of the degradation of GFP-250. COS-7 cells were transfected with GFP-250. (A) 48 h after transfection, cells were processed for immunofluorescence using antibodies to the α-subunit of the 20S proteasome, and imaged for GFP-250 and the proteasome. The proteasome is recruited to the GFP-250 aggresome. (B) 36 h after transfection, *clasto*-lactacystin β-lactone (10 μM) or media were added to the cells for 11 h. Cells were then imaged to localize the GFP chimera. The number of cells containing an aggresome is reported as percentage of transfected cells. 700 cells were counted for each condition. Proteasome inhibition causes an increase in GFP-250 aggresome formation. (C) COS-7 cells transfected for 12 h with GFP-250 were pulse labeled with [$^{35}$S]methionine for 1 h and then chased with unlabeled medium for the times indicated in the presence or absence of *clasto*-lactacystin β-lactone. The detergent soluble fractions were then immunoprecipitated with anti-p115 antibodies, separated by SDS-PAGE, and detected by fluorography. The gel was quantitatively evaluated by densitometry and presents percentage of radiolabeled GFP-250 remaining at each chase time point. Proteasome inhibition increases the half-life of GFP-250. Bar, 10 μm.

ubiquitin. As previously reported (Johnston et al., 1998), a high degree of colocalization of CFTR and ubiquitin was observed in the aggresome region (Fig. 5 B). Taken together, these results suggest that the proteasome is involved in the degradation of GFP-250 in an ubiquitin-independent manner. Although it has been shown that most proteins degraded by the proteasome are multiubiquitinated (reviewed in Hershko and Ciechanover, 1998), ubiquitin-independent proteasome degradation has been demonstrated for some proteins (Bercovich et al., 1989; Rosenberg-Hasson et al., 1989; Roberts, 1997).

### *Protein Aggregates Form at Cell Periphery and Move on Microtubules to the MTOC to Form the Aggresome*

Previous work has shown that the aggresome localizes to the MTOC and that nocodazole inhibits the process, but the dynamics of aggresome formation have not been studied. Using time-lapse imaging techniques in living cells, we followed the formation of aggresomes in COS-7 cells expressing GFP-250. Images were captured every 5–120 s for up to 130 min. A representative series of images showing aggresomal growth is shown in Fig. 8 A (see also accompanying QuickTime™ movie available at http://www.jcb.org/cgi/content/full/146/6/1239/F8/DC1). Small aggregates usually formed in the periphery of the cell and moved toward the MTOC in straight or curvilinear tracks. Occasionally, some of the particles moved in reverse directions. The speed of the particles was not constant over time. Particles usually moved in a discontinuous, stop and go manner. Fig. 8 B shows a tracing of a path taken by a representative particle moving towards the aggresome. The particle moved a total distance of 14.5 μm in 45 min, which represents an average speed of 0.32 μ/min, before merging with the aggresome.

To estimate the rate of aggresome growth, fluorescence intensity was measured in a region of interest (ROI) containing the juxtanuclear aggresomal compartment and normalized against total fluorescence. The total fluorescence remained constant over the time course of the experiment, suggesting that photobleaching was not significant during this interval. Each individual image was measured and plotted as a change of fluorescence intensity over time (Fig. 8 C). The increment in fluorescence intensity of the aggresome was linear over time, and after 120 min, the fluorescence intensity of the aggresome was doubled. Regression analysis ($r^2 = 0.98$) suggests that the process of aggresome formation follows a first order linear kinetics.

As previously shown, the microtubule depolymerizing drug nocodazole prevents the formation of perinuclear aggresomes and causes the formation of smaller protein ag-

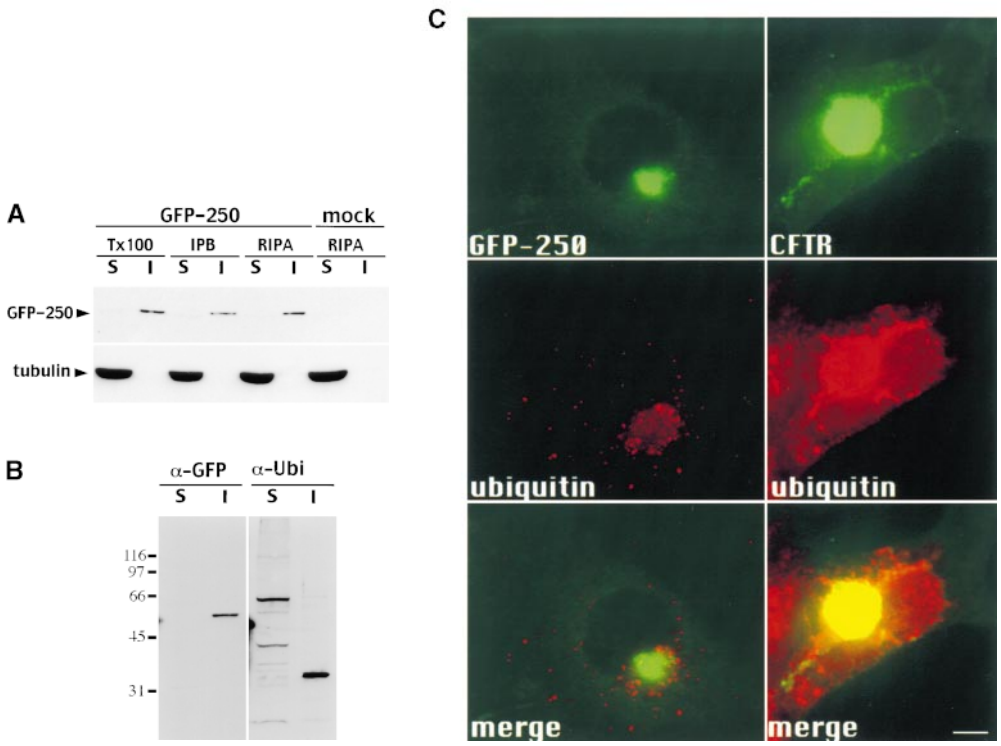


*Figure 7.* GFP-250 is not ubiquitinated. COS-7 cells were transfected with GFP-250. (A) 48 h after transfection, cells were extracted with Triton X-100, immunoprecipitation buffer (IPB) or RIPA (RIPA) buffer as in Methods, and the soluble (S) and insoluble (I) fractions separated by SDS-PAGE and immunoblotted with antibodies against GFP or tubulin. GFP-250 remains insoluble even under the most stringent extraction conditions. (B) 48 h after transfection, cells were extracted with Triton X-100, and the soluble (S) and insoluble (I) fractions were separated by SDS-PAGE and immunoblotted with antibodies against GFP. The membrane was then stripped and reprobed with anti-ubiquitin antibody. GFP-250 does not appear to be ubiquitinated. (C) 48 h after transfection, cells were processed for immunofluorescence using antibodies against ubiquitin, and imaged to localize GFP-250 and ubiquitin. Ubiquitin does not colocalize with GFP-250 aggresome. COS-7 cells were also transfected with CFTR and incubated with *clasto*-lactacystin β-lactone (10 μM) for 11 h after 36 h of transfection. Cells were processed for immunofluorescence using antibodies against CFTR and ubiquitin, and imaged to localize CFTR and ubiquitin. Ubiquitin does colocalize with the CFTR aggresome. Bar, 10 μm.

gregates dispersed in the periphery of the cells (Johnston et al., 1998). To show directly that the speed and path of particle delivery to the aggresome is affected by microtubule disruption, we incubated GFP-250–transfected COS-7 cells in the presence of nocodazole for 1 h at 4°C to depolymerize the microtubules. The cells were then shifted to 37°C and the aggresome dynamics were imaged. The behavior of a single representative particle over 360 s was analyzed in nocodazole-treated and control cells. As shown in Fig. 8 D, in untreated cells, the particle velocity oscillated between 0 and 0.25 μm/s. In cells treated with nocodazole, the particle velocity was dramatically decreased, oscillating between 0 and 0.03 μm/s, directly showing that particle movement responsible for aggresome growth is dependent on presence of intact microtubules.

At any given time point, a significant percentage of the particles were either moving very slowly or not moving at all. A population analysis of 10 particles over 35 time points (total ~350 events) indicated a tailed distribution of movement speeds, with ~50% of the events occurring between 0 and 0.025 μm/s (Fig. 8 E, black bars). This distribution was dramatically altered in cells incubated with nocodazole. After 1 h of nocodazole incubation, 99% of the movement events occurred at speeds between 0 and 0.025 μm/s (Fig. 8 E, gray bars). Although some of the particles moved at speeds comparable to those in control cells, the movement was never directional, and none of the particles analyzed moved >0.5 μm over a period of 30 min (compare with 14.5 μm in Fig. 8 B). Taken together, these results indicate that perinuclear aggresomes form by the movement of peripherally nucleated smaller particles towards the MTOC.

### *Disruption of the Dynein/Dynactin Complex Inhibits Formation of the Aggresome*

The loss of motility of peripheral aggregates after nocodazole treatment suggests that a microtubule-dependent motor might be involved in their minus-end–directed movement to the MTOC. The vast majority of minus-end–directed transport processes in interphase cells require dynein, which is typically associated with dynactin. Cytoplasmic dynein has been implicated in the distribution of late endosomes and lysosomes, and the centrosomal localization of the Golgi complex, as well as the retrograde transport of membranous organelles in axons, vesicular transport from early to late endosomes, and traffic to the Golgi of pre-Golgi intermediates (reviewed in Vallee and Sheetz, 1996; Hirokawa, 1998). Although molecular motors have been clearly implicated in transport of membrane bound organelles, much less is known about the microtubule-dependent interaction of motors with membrane free particles. Dynein/dynactin-associated minus-end motor activity can be experimentally inhibited by overexpressing the p50/dynamitin component of the dynactin complex (Echeverri et al., 1996; Burkhardt et al., 1997; Presley et al., 1997). To test if the dynactin complex is involved in the transport of peripheral aggregates to the MTOC, we

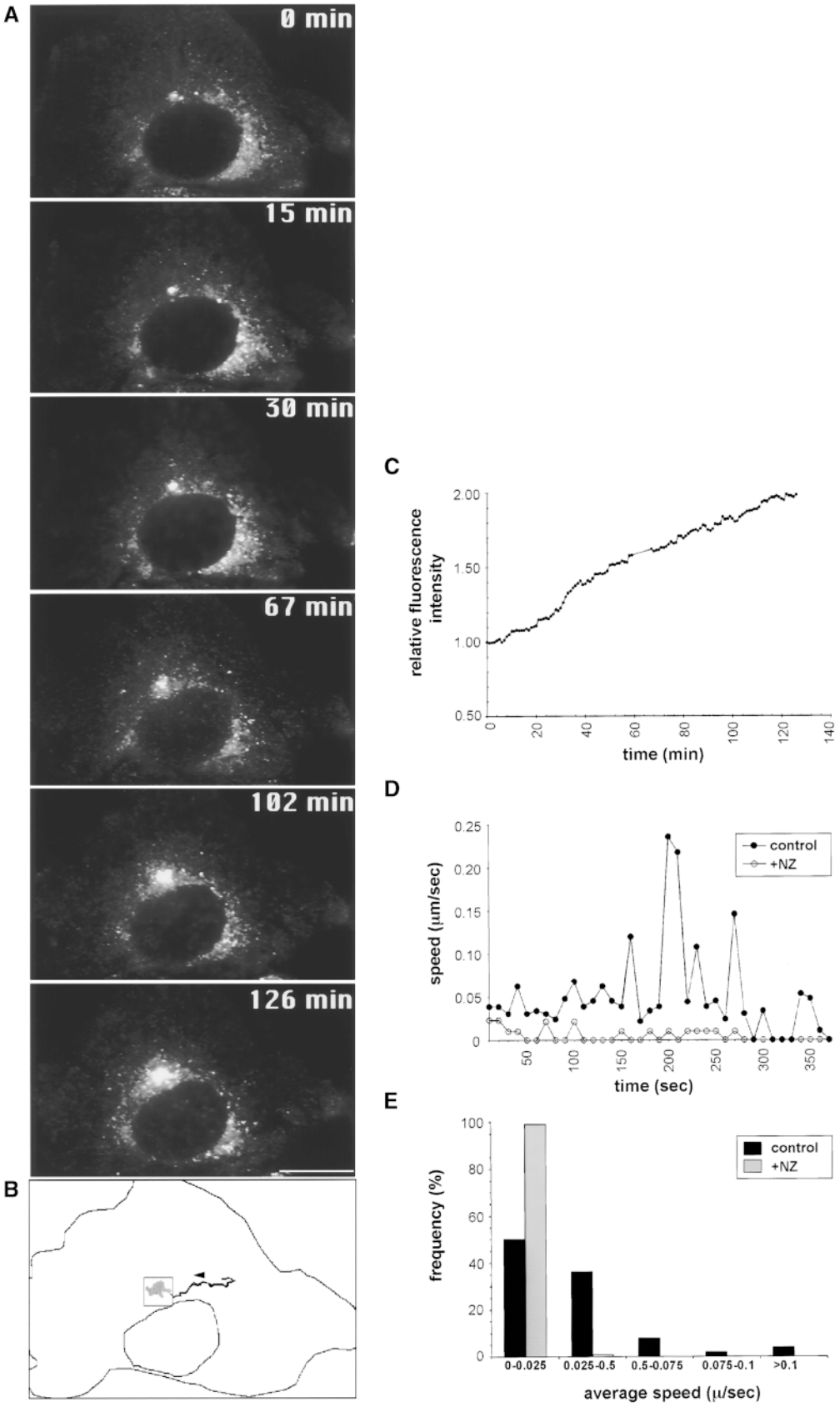


*Figure 8.* Dynamics of aggresome formation. COS-7 cells were transfected with GFP-250 and 48 h later imaged every 60 s for 120 min. (A) Image series showing aggresome formation. Accompanying QuickTime™ movie shows aggresome progression between 60 and 120 min (video available at http://www.jcb.org/cgi/content/full/146/6/1239/F8/DC1). (B) Path taken by a representative particle en route to the aggresome. One particle was followed over a period of 45 min until it disappeared into the aggresome. (C) Fluorescent intensities associated with the aggresome region of interest (ROI) for the cell shown in A are plotted at 60-s intervals. ROI is marked in B by a gray square. (D) Particle velocity in control (closed circles) and in nocodazole-treated (open circles) cells. Transfected cells were incubated with 10 μg/μl of nocodazole for 1 h at 4°C, then returned to 37°C and imaged every 10 s. (E) Population analysis of motile particles in control (black bars) and nocodazole-treated (gray bars) cells. Velocities of 10 different particles were measured, grouped into 0.025-μm/s intervals, and plotted. Representative traces of one particle for each condition are shown. Bar, 10 μm.

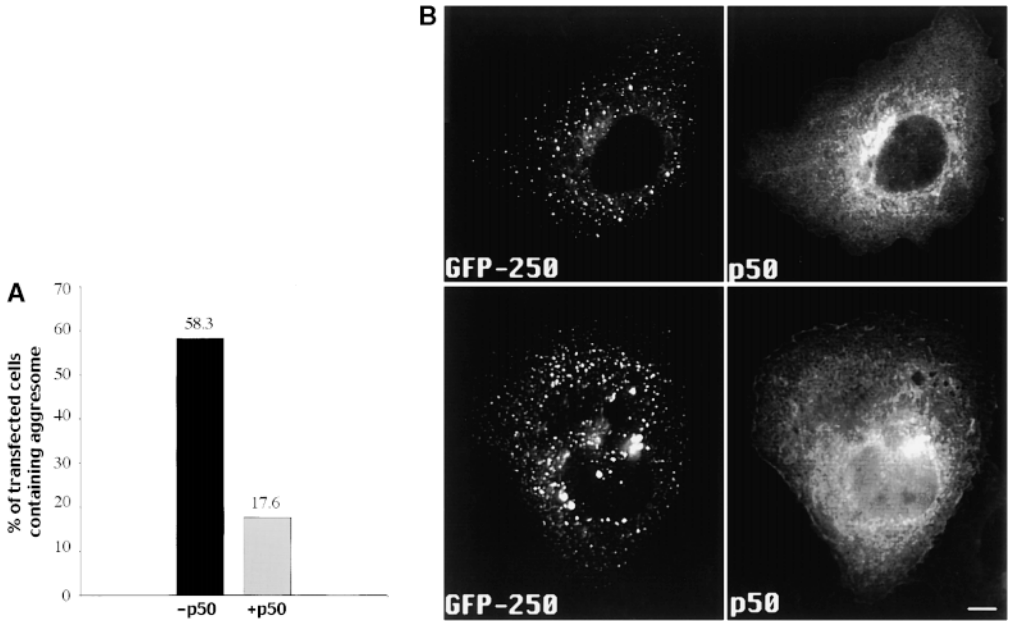


*Figure 9.* p50/dynamitin overexpression inhibits aggresome formation. COS-7 cells were either transfected with GFP-250 or cotransfected with GFP-250 and p50/dynamitin in a 1:2 ratio. 48 h after transfection, cells were processed for immunofluorescence using antibodies against p50/dynamitin, and imaged to localize the GFP-250 and p50/dynamitin. The number of cells containing an aggresome in cells transfected only with GFP-250 (302 cells counted) and in cotransfected cells (143 cells counted) were counted and are expressed as percentage of transfected cells. Cells expressing p50/dynamitin show significant reduction in aggresome formation. B shows two representative examples of cells expressing high levels of p50/dynamitin, in which only small peripheral particulates can be seen. The results are from three independent experiments. Bar, 10 μm.

cotransfected COS-7 cells with GFP-250 and p50/dynamitin and examined the formation of aggresomes in cells expressing both proteins. As shown in Fig. 9 A, ~58% of control cells (302 cells counted) transfected only with GFP-250 formed an aggresome, but only ~18% of cells cotransfected with GFP-250 and p50/dynamitin and expressing high levels of p50/dynamitin (143 cells counted) showed aggresome formation. In most of the cotransfected cells, small GFP-250 aggregates were detected, but remained in the periphery of the cell (Fig. 9 B). Aggresomes did form in a proportion of cells expressing p50/dynamitin, and this is most likely due to incomplete inactivation of the dynactin complex. Alternatively, since aggresome formation can take <2 h, some cells could form an aggresome before a significant level of dynactin inactivation was achieved. However, the significant inhibitory effect of p50/dynamitin overexpression suggests that the translocation of peripheral GFP-250 aggregates to the MTOC is powered by the microtubule motor complex of dynein/dynactin.

### *Formation of Aggresomes Displaces Golgi Elements and Causes Reorganization of Pericentral Microtubules but Does Not Disrupt ER to Golgi Traffic*

The aggresome is localized to the region of the cell usually occupied by the Golgi complex and as already shown in Fig. 1 F, aggresome formation interferes with proper Golgi localization. We investigated this phenomenon in more detail, and found that aggresome size is inversely correlated with proper Golgi localization, that is, as the aggresome grows, the Golgi becomes more disorganized and distorted around the aggresome (Fig. 10 A). It appears that the aggresome forms a physical barrier between the Golgi cisternal elements and the MTOC around which they are usually arranged.

Similarly, microtubules, which are normally assembled and radiate from the central MTOC (Osborn and Weber, 1976; Kristofferson et al., 1986), are distorted in cells containing large aggresomes (Fig. 10 B). Instead of the normal astral distribution, a central hole containing the aggresome is visible in most cells. More peripherally distributed MTs appear normal.

Many studies have shown that Golgi disruption or changes in MT organization can cause defects in protein transport (Dascher and Balch, 1994; Wilson et al., 1994; Cole et al., 1996). To determine if protein transport was affected by the cellular changes accompanying aggresome formation, we analyzed the transport of a marker protein, the G protein of the vesicular stomatitis virus (VSV-G), in aggresome containing cells. COS-7 cells were first transfected with GFP-250 for 48 h to promote aggresome formation. Cells were then infected with a temperature-sensitive strain (VSVts045) of the virus (Gallione and Rose, 1985) at the nonpermissive temperature of 42°C, and incubated at this temperature for 3 h. This leads to the synthesis and accumulation of the VSV-G protein in the ER but does not allow further entry of the VSV-G protein into the secretory pathway (De Silva et al., 1990, 1993; Hammond and Helenius, 1994). To allow transport of VSV-G protein out of the ER, cells are shifted to the permissive temperature of 32°C. The movement of the VSV-G protein from the ER into the Golgi and later to the cell surface can be followed by immunofluorescence at different time points after the temperature shift. As shown in Fig. 10 C, an untransfected cell and a transfected cell containing a relatively large GFP-250 aggresome have been infected at the nonpermissive temperature and contain VSV-G protein

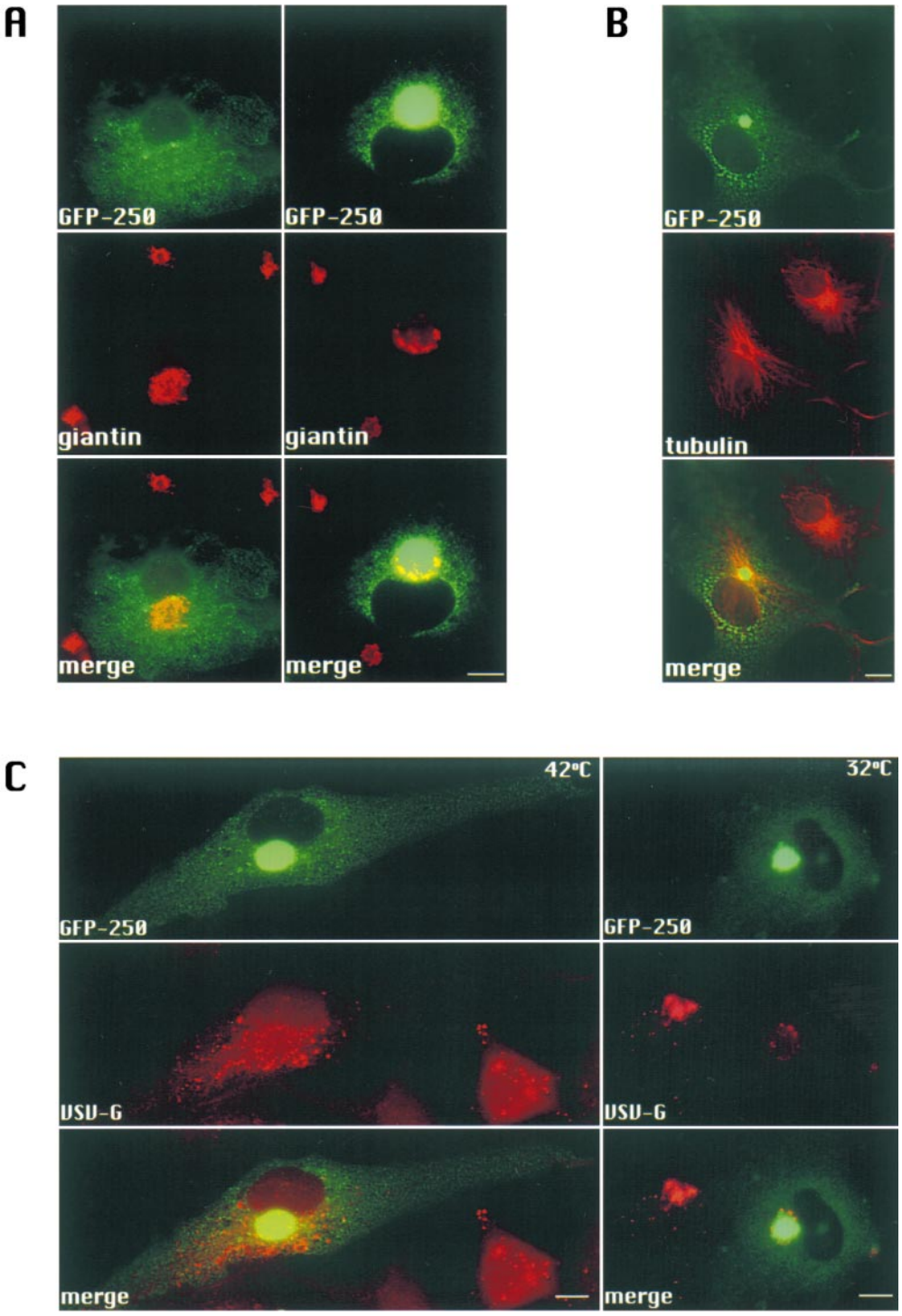


*Figure 10.* Disruption of the Golgi complex and microtubules does not overtly inhibit ER to Golgi transport. COS-7 cells were transfected with GFP-250. (A and B) 48 h after transfection, cells were processed for immunofluorescence using antibodies against giantin (A) or tubulin (B), and imaged to localize the GFP-250 and giantin or tubulin. Giantin is progressively displaced by the forming GFP-250 aggresome. Microtubule structure is perturbed and microtubules surround the aggresome. (C) 48 h after transfection, cells were infected with VSVtsO45 at the nonpermissive temperature of 42°C. Cells were either maintained at 42°C or shifted to the permissive temperature of 32°C for 1 h. Cells were then processed for immunofluorescence using antibodies against VSV-G protein, and imaged to localize the GFP chimera and the VSV-G protein. In untransfected cells as well as in cells containing an aggresome, VSV-G protein was delivered to the Golgi complex. Bars, 10 μm.

within the ER. This represents the starting point of the transport. Such cells were then shifted to the permissive temperature of 32°C for 1 h. In both the untransfected cell and in the aggresome containing cell, the VSV-G protein is transported from the ER to the Golgi. Interestingly, although the Golgi is displaced around the aggresome, it appears functionally competent for protein transport in a manner analogous to that in infected cells not containing an aggresome. Even though changes in transport kinetics can not be excluded at this point, the data suggest that ER to Golgi transport of cargo proteins is not overtly inhibited by formation of the aggresome.

## *Discussion*

A recent report has described the initial characterization of a novel subcellular structure, the aggresome (Johnston et al., 1998). Aggresomes form by the deposition of mis-

folded proteins in a large structure surrounding the MTOC. The initial report documented the formation of aggresomes in cells expressing CFTR or PS1, two integral membrane proteins that span the membrane multiple times. In both cases, treating cells with compounds that inhibit proteasome activity significantly increased the formation of aggresomes. Based on these results, it was proposed that aggresome formation represents a general cellular response to aggregated proteins.

### *Generality of Aggresome Formation*

To examine the generality of this cellular response, we analyzed whether cells expressing various chimeric proteins encoding the entire sequence of the soluble protein GFP fused in frame to various coding regions of the cytosolic protein p115 form aggresomes. GFP chimeras containing the entire coding region of p115 or the $NH_2$-terminal 3/4 portion of p115 did not form aggresomes and were targeted to the expected cellular localization, the Golgi. In contrast, a chimera containing only the $NH_2$-terminal 250 amino acids of p115 aggregated into insoluble particles and was deposited within an aggresomal structure. Interestingly, the location of the 250 amino acid p115 sequence relative to the GFP was critical for aggresome formation: aggresomes formed only when GFP preceded the p115 sequence, whereas the reverse construct was not misfolded and did not lead to aggresome deposition. It must be stressed that GFP-250 was at least partially folded since the GFP moiety was fluorescent, suggesting that the p115 sequence was misfolded to expose hydrophobic domains capable of aggregation. Hydropathy plot of the $NH_2$-terminal 250–amino acid region of p115 shows many hydrophobic side chains and it is likely that synthesis of only a portion of the globular head region of p115 prevents correct intramolecular folding and leads to aggregation. The GFP-250 aggresome was morphologically indistinguishable from that formed by CFTR and PS1, suggesting that cytosolic proteins can also form aggresomes and supporting the hypothesis that formation of aggresomes is a general cellular response when the degradative capacity of a cell is overtaxed.

### *Dynamics of Aggresome Formation*

The previous report documented that aggresomes localize to the MTOC and that treatment of cells with nocodazole prevents aggresome formation (Johnston et al., 1998). We used time-lapse imaging to obtain quantitative measurements of aggresome formation. Aggresome precursors seem to nucleate throughout the cells, most likely during translation of nascent chains on polysomes. As described previously, the high effective concentration of nascent polypeptides during biosynthesis due to macromolecular crowding could stimulate aggregation (Hartl, 1996). Aggregate particles move towards the MTOC at speeds exceeding those of simple diffusion. The movement is directly correlated with intact microtubules, and particles do not move in nocodazole-treated cells. The speed of particles appears comparable to that measured for different motor families involved in a variety of cellular functions (reviewed in Howard, 1997). The nature of the motor activity involved in aggresome formation was investigated by overexpressing the p50/dynamatin subunit of the dynein/dynactin complex. The observed inhibition in aggresome formation suggests that dynein/dynactin plays a key role in the translocation of peripheral aggregates to the MTOC where they form the aggresome.

### *Aggresome Content*

Ultrastructural examination of aggresomes indicates a complex architecture of individual particles interspersed with subcellular organelles and filaments, and surrounded by membranous organelles and vimentin fibers. The organelles within the aggresome appear to be predominantly mitochondria and lysosomes. Surrounding the aggresome are other membranes, including the Golgi. At the molecular level, the aggregated protein appears to recruit cellular chaperones to the aggresome. This is not unexpected since chaperones are known to be associated with misfolded proteins and aid in their presentation for degradation (Hartl, 1996). It is possible that members of the Hsp70 and the chaperonin family may play a role in GFP-250 degradative pathway. Interestingly, whereas two members of the Hsp40 family (Hdj1 and Hdj2) and a chaperonin (TCP1) were associated with particles throughout the aggresome, Hsc70 was localized in a ring structure around the aggresome but was not concentrated within the aggresome interior. The rationale for this differential distribution is currently unknown but might reflect sequential participation of the different chaperones.

One of the most effective ways to prevent aggregation is to rapidly target the misfolded protein to degradation. In agreement, our data show that the proteasome is recruited to the GFP-250 aggresome. Similar results were obtained during CFTR overexpression and aggresome formation in a recently published manuscript (Wigley et al., 1999). Degradation of most proteins by the proteasome requires the covalent conjugation of ubiquitin chains, which target the protein to degradation (reviewed by Hershko and Ciechanover, 1998). Interestingly, our data suggest that although the proteasome is responsible for GFP-250 degradation, GFP-250 is not ubiquitinated. Previous studies have reported ubiquitin-independent proteasomal degradation (Bercovich et al., 1989; Rosenberg-Hasson et al., 1989; Roberts, 1997).

### *Effect of Aggresome on Cellular Structure and Function*

Formation of aggregates of misfolded protein within specialized cells has been linked to a number of pathological states (Sipe, 1992; Thomas et al., 1995; Carrell and Lomas, 1997). However, whether the deposition of a protein causes secondary cellular problems is less well understood. We have examined the overall distribution of a number of subcellular organelles and found that the Golgi complex and the arrangement of microtubules are disrupted by aggresome formation. Instead of the normally compact Golgi structure surrounding the MTOC, the Golgi elements were dispersed around the aggresome. Similarly, microtubular networks were partially disorganized, with microtubules surrounding the aggresome, instead of originating from the MTOC. However, despite these changes,

the cells exhibited many normal processes. Specifically, viral infection and subsequent viral protein synthesis and targeting appeared normal, as did the retention of the viral transmembrane G protein within the ER at nonpermissive temperature. The temperature-sensitive VSV-G protein can not fold properly and is retained within the ER membrane 42°C. When the temperature is shifted to 32°C the G protein folds correctly, exits the ER, and is transported to the Golgi. All the processes of protein synthesis and quality control operational within normal cells were also operational in cells containing large aggresomes. Similarly, the traffic from the ER to the Golgi appeared relatively normal in aggresome-containing cells. Whereas we can not currently exclude changes in the rate or efficiency of transport, it appears that presence of a large aggresomal structure within a cell does not negatively influence at least some of their physiological processes. It seems that the segregation of the aggregated proteins into a single structure might, in fact, sequester problematic proteins and thereby maintain relatively normal cellular milieu. That the cells retain capacity for normal life is also suggested by the finding that the life spans of cells containing aggresomes were not fundamentally different from normal cells (data not shown). These results suggest that pathology in cells containing aggregated proteins is probably not due to having an aggresome that inhibits vital cellular functions, but is more related to the functional unavailability of the aggregated protein.

We are most grateful to Mr. Edward Phillips and Mr. Albert Tousson for their help with electron microscopic and time-lapse imaging techniques. We wish to thank Dr. Douglas Cyr and Geoffrey Meacham for the kind gift of antibodies against ubiquitin, Hdj1, Hdj2, TCP1, and Hsp70. We also thank Dr. Hans Peter Hauri for anti-giantin antibodies and Dr. Bill Britt for anti-vimentin antibodies. We are grateful to Nicole Faulkner and Dr. Richard Vallee for pCMVH50-myc cDNA and mAb 50.1, and for technical advice. We wish to thank Dr. C. Alvarez for valuable comments on the manuscript.

Submitted: 23 April 1999
Revised: 27 July 1999
Accepted: 18 August 1999

### *References*

Barroso, M., D.S. Nelson, and E. Sztul. 1995. Transcytosis-associated protein (TAP)/p115 is a general fusion factor required for binding of vesicles to acceptor membranes. *Proc. Natl. Acad. Sci. USA*. 92:527–531.

Bercovich, Z., Y. Rosenberg-Hasson, A. Ciechanover, and C. Kahana. 1989. Degradation of ornithine decarboxylase in reticulocyte lysate is ATP-dependent but ubiquitin-independent. *J. Biol. Chem*. 264:15949–15952.

Bonifacino, J.S., C.K. Suzuki, J. Lippincott-Schwartz, A.M. Weissman, and R.D. Klausner. 1989. Pre-Golgi degradation of newly synthesized T cell antigen receptor chains: intrinsic sensitivity and the role of subunit assembly. *J. Cell Biol.* 109:73–83.

Burkhardt, J.K., C.J. Echeverri, T. Nilsson, and R.B. Vallee. 1997. Overexpression of the dynamitin (p50) subunit of the dynactin complex disrupts dynein-dependent maintenance of membrane organelle distribution. *J. Cell Biol.* 139:469–484.

Carey, K.L., S.A. Richards, K.M. Lounsbury, and I.G. Macara. 1996. Evidence using a green fluorescent protein-glucocorticoid receptor chimera that the Ran/TC4 GTPase mediates an essential function independent of nuclear protein import. *J. Cell Biol.* 133:985–996.

Carrell, R.W., and D.A. Lomas. 1997. Conformational disease. *Lancet.* 350: 134–138.

Cole, N.B., N. Sciaky, A. Marotta, J. Song, and J. Lippincott-Schwartz. 1996. Golgi dispersal during microtubule disruption: regeneration of Golgi stacks at peripheral endoplasmic reticulum exit sites. *Mol. Biol.Cell.* 7:631–650.

Cubitt, A.B., R. Heim, S.R. Adams, A.E. Boyd, L.A. Gross, and R.Y. Tsien. 1995. Understanding, improving and using green fluorescent proteins. *Trends Biochem. Sci.* 20:448–455.

Cyr, D.M. 1997. The Hsp40 (DnaJ-related) family of proteins. *In* Guidebook to Molecular Chaperones and Protein Folding Factors. Gething, M.J. editor. Sambrook & Tooze at Oxford University Press, Oxford, UK. 89–95.

Dascher, C., and W.E. Balch. 1994. Dominant inhibitory mutants of ARF1 block endoplasmic reticulum to Golgi transport and trigger disassembly of the Golgi apparatus. *J. Biol. Chem*. 269:1437–1448.

De Silva, A.M., W.E. Balch, and A. Helenius. 1990. Quality control in the endoplasmic reticulum: folding and misfolding of vesicular stomatitis virus G protein in cells and in vitro. *J. Cell Biol*. 111:857–866.

De Silva, A., I. Braakman, and A. Helenius. 1993. Posttranslational folding of vesicular stomatitis virus G protein in the ER: involvement of noncovalent and covalent complexes. *J. Cell Biol.* 120:647–655.

Dobson, C.M., and R.J. Ellis. 1998. Protein folding and misfolding inside and outside the cell *EMBO (Eur. Mol. Biol. Organ.) J.* 17:5251–5254.

Echeverri, C.J., B.M. Paschal, K.T. Vaughan, and R.B. Vallee. 1996. Molecular characterization of the 50-kD subunit of dynactin reveals function for the complex in chromosome alignment and spindle organization during mitosis. *J. Cell Biol.* 132:617–633.

Ellis, R.J., and F.U. Hartl. 1996. Protein folding in the cell: competing models of chaperonin function. *FASEB J.(Fed. Am. Soc. Exp. Biol.)* 10:20–26.

Frydman, J., and J. Hohfeld. 1997. Chaperones get in touch: the hip-hop connection. *Trends Biochem. Sci.* 22:87–92.

Gallione, C.J., and J.K. Rose. 1985. A single amino acid substitution in a hydrophobic domain causes temperature-sensitive cell-surface transport of a mutant viral glycoprotein. *J. Virol.* 54:374–382.

Glotzer, M., A.W. Murray, and M.W. Kirschner. 1991. Cyclin is degraded by the ubiquitin pathway. *Nature*. 349:132–138.

Hammond, C., and A. Helenius. 1994. Quality control in the secretory pathway: retention of a misfolded viral membrane glycoprotein involves cycling between the ER, intermediate compartment, and Golgi apparatus. *J. Cell Biol.* 126:41–52.

Hartl, F.U. 1996. Molecular chaperones in cellular protein folding. *Nature*. 381: 571–580.

Hershko, A., and A. Ciechanover. 1998. The ubiquitin system. *Annu. Rev. Biochem*. 67:425–479.

Hirokawa, N. 1998. Kinesin and dynein superfamily proteins and the mechanism of organelle transport. *Science*. 279:519–526.

Hohfeld, J., and S. Jentsch. 1997. Grpe-like regulation of the Hsc70 chaperone by the anti-apoptotic protein Bag-1. *EMBO (Eur. Mol. Biol. Organ.) J.* 16: 6209–6216.

Howard, J. 1997. Molecular motors: structural adaptations to cellular functions. *Nature.* 389:561–567.

Hurle, M.R., L.R. Helms, L. Li, W. Chan, and R. Wetzel. 1994. A role for destabilizing amino acid replacements in light-chain amyloidosis. *Proc. Natl. Acad. Sci. USA*. 91:5446–5450.

Jaenicke, R. 1991. Protein folding: local structures, domains, subunits, and assemblies. *Biochemistry*. 30:3147–3161.

Jensen, T.J., M.A. Loo, S. Pind, D.B. Williams, A.L. Goldberg, and J.R Riordan. 1995. Multiple proteolytic systems, including the proteasome, contribute to CFTR processing. *Cell.* 83:129–135.

Johnston, J.A., C.L. Ward, and R.R. Kopito. 1998. Aggresomes: A cellular response to misfolded proteins. *J. Cell Biol.* 143:1883–1898.

Kain, S.R., M. Adams, A. Kondepudi, T.T. Yang, W.W. Ward, and P. Kitts. 1995. Green fluorescent protein as a reporter of gene expression and protein localization. *Biotechniques*. 19:650–655.

Kopito, R.R. 1997. ER quality control: the cytoplasmic connection. *Cell.* 88: 427–430.

Kristofferson, D., T. Mitchison, and M. Kirschner. 1986. Direct observation of steady-state microtubule dynamics. *J. Cell Biol.* 102:1007–1019.

Kubota, H., G. Hynes, and K. Willison. 1995. The chaperonin containing t-complex polypeptide 1 (TCP-1). Multisubunit machinery assisting in protein folding and assembly in the eukaryotic cytosol. *Eur. J. Biochem*. 230:3–16.

Linstedt, A.D., and H.P. Hauri. 1993. Giantin, a novel conserved Golgi membrane protein containing a cytoplasmic domain of at least 350 kDa. *Mol. Biol. Cell*. 4:679–693.

Marshall, J., R. Molloy, G.W. Moss, J.R. Howe, and T.E. Hughes. 1995. The jellyfish green fluorescent protein: a new tool for studying ion channel expression and function. *Neuron*. 14:211–215.

Meacham, G.C., Z. Lu, S. King, E. Sorscher, A. Tousson, and D.M. Cyr. 1999. The Hdj-2/Hsc70 chaperone pair facilitates early steps in CFTR biogenesis. *EMBO (Eur. Mol. Biol. Organ.) J.* 18:1492–1505.

Morimoto, R.I., A. Tissieres, and C. Georgopoulos, editors. 1990. Stress Proteins in Biology and Medicine. Cold Spring Harbor Laboratory Press, Cold Spring Harbor, New York. 450 pp.

Nakamura, N., M. Lowe, T.P. Levine, C. Rabouille, and G. Warren. 1997. The vesicle docking protein p115 binds GM130, a cis-Golgi matrix protein, in a mitotically regulated manner. *Cell*. 89:445–455.

Nelson, D.S., C. Alvarez, Y.S. Gao, R. Garcia-Mata, E. Fialkowski, and E. Sztul. 1998. The membrane transport factor TAP/p115 cycles between the Golgi and earlier secretory compartments and contains distinct domains required for its localization and function. *J. Cell Biol.* 143:319–331.

Ogawa, H., S. Inouye, F.I. Tsuji, K. Yasuda, and K. Umesono. 1995. Localization, trafficking, and temperature-dependence of the Aquorea green fluorescent protein in cultured vertebrate cells. *Proc. Natl. Acad. Sci. USA*. 92: 11899–11903.

Osborn, M., and K. Weber. 1976. Cytoplasmic microtubules in tissue culture cells appear to grow from an organizing structure towards the plasma membrane. *Proc. Natl. Acad. Sci. USA*. 73:867–871.

Presley, J.F., N.B. Cole, T.A. Schroer, K. Hirschberg, K.J. Zaal, and J. Lippincott-Schwartz. 1997. ER-to-Golgi transport visualized in living cells. *Nature*. 389:81–85.

Rizzuto, R., M. Brini, F. De Giorgi, R. Rossi, R. Heim, R.Y. Tsien, and T. Pozzan. 1996. Double labeling of subcellular structures with organelle-targeted GFP mutants in vivo. *Curr. Biol.* 6:183–188.

Roberts, B.J. 1997. Evidence of proteasome-mediated cytochrome P-450 degradation. *J. Biol. Chem*. 272:9771–9778.

Rosenberg-Hasson, Y., Z. Bercovich, A. Ciechanover, and C. Kahana. 1989. Degradation of ornithine decarboxylase in mammalian cells is ATP dependent but ubiquitin independent. *Eur. J. Biochem*. 185:469–474.

Sapperstein, S.K., D.M. Walter, A.R. Grosvenor, J.E. Heuser, and M.G. Waters. 1995. p115 is a general vesicular transport factor related to the yeast endoplasmic reticulum to Golgi transport factor Uso1p. *Proc. Natl. Acad. Sci. USA*. 92:522–526.

Sipe, J.D. 1992. Amyloidosis. *Annu. Rev. Biochem*. 61:947–975.

Takayama, S., D.N. Bimston, S. Matsuzawa, B.C. Freeman, C. Aime-Sempe, Z. Xie, R.I. Morimoto, and J.C. Reed. 1997. BAG-1 modulates the chaperone activity of Hsp70/Hsc70. *EMBO (Eur. Mol. Biol. Organ.) J.* 16:4887–4896.

Thomas, P.J., B.H. Qu, and P.L. Pedersen. 1995. Defective protein folding as a basis of human disease. *Trends in Biochem. Sci.* 20:456–459.

Tsien, R.Y. 1998. The green fluorescent protein. *Annu. Rev. Biochem*. 67:509–544.

Vallee, R.B., and M.P. Sheetz. 1996. Targeting of motor proteins. *Science*. 271: 1539–1544.

Ward, C.L., and R.R. Kopito. 1994. Intracellular turnover of cystic fibrosis transmembrane conductance regulator. Inefficient processing and rapid degradation of wild-type and mutant proteins. *J. Biol. Chem*. 269:25710–25718.

Ward, C.L., S. Omura, and R.R. Kopito. 1995. Degradation of CFTR by the ubiquitin-proteasome pathway. *Cell*. 83:121–127.

Waters, M.G., D.O. Clary, and J.E. Rothman. 1992. A novel 115-kD peripheral membrane protein is required for intercisternal transport in the Golgi stack. *J. Cell Biol.* 118:1015–1026.

Wetzel, R. 1994. Mutations and off-pathway aggregation of proteins. *Trends Biotechnol*. 12:193–198.

Wigley, W.C., R.P. Fabunmi, M.G. Lee, C.R. Marino, S. Muallem, G.N. DeMartino, and P.J. Thomas. 1999. Dynamic association of proteasomal machinery with the centrosome. *J. Cell Biol.* 145:481–490.

Wilson, B.S., C. Nuoffer, J.L. Meinkoth, M. McCaffery, J.R. Feramisco, W.E. Balch, and M.G. Farquhar. 1994. A Rab1 mutant affecting guanine nucleotide exchange promotes disassembly of the Golgi apparatus. *J. Cell Biol.* 125:557–571.

Zimmerman, S.B., and A.P. Minton. 1993. Macromolecular crowding: biochemical, biophysical, and physiological consequences. *Annu. Rev. Biophys. Biomol. Struct.* 22:27–65.